ELSEVIER

Polymer 41 (2000) 5885–5893

polymer

Determination of pore size distribution for mesoporous materials and polymeric gels by means of DSC measurements: thermoporometry

M. Iza[a], S. Woerly[b], C. Danumah[a], S. Kaliaguine[a], M. Bousmina[a,*]

[a]*Department of Chemical Engineering, CERSIM, Laval University, Québec, Que., Canada G1K 7P4*
[b]*Organogel Canada Ltée. Parc Technologique du Québec Métropolitain, 1400, bureau 205, Québec, Que., Canada G1P 4R7*

Received 8 July 1999; received in revised form 30 September 1999; accepted 15 October 1999

Abstract

The determination of porous structure of fragile materials from classical methods such as mercury porosimetry and nitrogen adsorption–desorption methods is often delicate and can be source of false structure interpretation. The thermoporometry is an alternative method, sometimes the unique method, allowing a better characterization of porous fragile and soft materials and hydrogels.

In this paper we report on the use of thermoporometry as a technique allowing the determination of pore size distribution in mesoporous materials. First, the reliability of the technique was tested on rigid mesoporous silica with known pore size distribution. The expected pore radius distribution curve was obtained. Thereafter, the technique was applied to characterize the mesoporous structure of poly(*N*-(2-hydroxypropyl) methacrylamide) (PHPMA) gels swollen in aqueous medium. The pore size distributions determined were compared to those obtained from nitrogen physisorption isotherms.

Keywords: DSC; Hydrogels; Mesopore

1. Introduction

Polymeric porous materials are systems of great interest in many industrial applications including biomedical, pharmaceutical, super-absorbents and membranes. Their use is in constant progress as demonstrated by numerous published papers in this field.

The performances and the capacity of these systems to absorb a liquid are directly related to their mesoporous structure and their high specific surface area. These properties are usually suited for medical applications. Hydrogels are polymer networks that can swell in hydrophilic solvents or biological fluids. Their beneficial properties such as biocompatibility and low mechanical irritation [1] make them good candidates for applications such as controlled-release pharmaceuticals and surgical implants [2].

Various techniques were used to characterize the porous structure of these materials. Some of the widely used methods are mercury porosimetry and the nitrogen adsorption–desorption equilibrium using the Barrett–Joyner–Halenda method (BJH). However, these techniques require a dry sample and thus are inadequate for hydrogels. Desiccation of the hydrogels that are fragile and soft may, indeed, induce dramatic modifications on the material morphology and its pore size distribution. The determination of porosity by means of these techniques may be, in these cases, inappropriate and the obtained results do not reflect the actual structure of the gel under its use conditions. An alternative method was suggested by Kuhn et al. [3]. The authors reported that the dependence of the freezing point on the size of microcrystals could provide a method for the determination of the ultrastructure of porous systems. Using this concept, Defay et al. [4] established a theoretical background for the phase behavior (thermodynamic equilibrium between gas, liquid and solid phases) of a liquid held inside a porous material taking into account the effect of the curvature of the interfaces between the three phases. In the classical treatment of thermodynamic equilibrium between two phases such as liquid–gas or solid–liquid it is implicitly supposed that the interface is infinitely flat (a mathematical plane) and all the molecules have the same probability to cross the interface from one phase to another. However, if the interface is curved, the topological environment and the ability of the molecules to diffuse from one phase to another (to increase their entropy) is directly related to the local curvature of the interface. The interfacial tension and the difference in pressure across the interface have to be considered. This introduces a supplementary equation (Laplace equation) on the classical Gibbs–Duhem equations for the

* Corresponding author. Fax: +1-418-656-5993.
E-mail address: bousmina@gch.ulaval.ca (M. Bousmina).

0032-3861/00/$ - see front matter
PII: S0032-3861(99)00776-4

phase equilibrium. Laplace equation involves the principal radii of the interface curvature and thus the knowledge of the other thermodynamic parameters allows the determination of the curvature radius and the size of the pores in a porous material. The principle of the method is based on the lowering of the triple point temperature of a liquid filling a porous material. The triple point temperature of these systems depends on the solid–liquid and the liquid–gas interfaces. Thus, the shift in equilibrium temperature of the liquid–solid transformation allows the determination of the pore size distribution, porous volume and the total surface area of the structured material. Additionally, the shape of the mesopores can be estimated from this technique by comparing the corresponding crystallization and fusion thermograms [5].

Since the studies of Brun et al. [6], this technique has been successfully applied to a large number of porous materials: alumina [6], silica gel [7], resins [8,9], butyl rubber [10], titania gels [11] and rubber grade carbon blacks [12]. However, despite the success obtained by thermoporometry, to the best of our knowledge this technique has never been applied to polymeric hydrogels. Technical consideration of this method especially the freezing process has been recently reviewed by Scherer [13].

This work complements former studies carried out by Woerly et al. [14]. The authors studied the structure of poly[*N*-(2-hydroxypropyl) methacrylamide] hydrogels (PHPMA) by mercury porosimetry and scanning electron microscopy. It was found that the PHPMA gel presents a macrophase-separated structure. The bulk of the gel constitutes a colloidal-type structure forming a three-dimensional network of microspheres of 3–5 μm in a loosely packed contact. The limit of the pore system was represented by the contiguity of the surface of the spheres, while the effective surface area of the hydrogel was found to be a function of the mesopores present at the surface of the spheres. The mercury porosimetry revealed that the largest fraction of the total pore volume of the gel is occupied by pores of dimensions 10–50 μm in diameter.

In this work, the mesoporous structure of a PHPMA hydrogel was probed by differential scanning calorimetry (DSC). DSC was used to determine the solidification thermogram of PHPMA hydrogel saturated by water. The pore radius distribution curve was determined and compared to the pore radius distribution obtained from the BJH treatment of nitrogen physisorption isotherms at 77 K.

2. Theoretical background

As discussed in Section 1, the triple point temperature of a solvent saturating a porous material depends on the pore size of this material. A basic form of this dependence consists of extending the Kelvin equation for capillary condensation to liquid–solid transformation by considering that the crystal induces a thermodynamic perturbation on the phase equilibrium in the same fashion, as does a drop of the same dimensions [4]. Under this condition, Kelvin equation for liquid–solid transformation writes

$$\ln(T/T_0) = \frac{2v_l\gamma_{ls}}{R_p\Delta H_0} \tag{1}$$

This equation is also known in the following approximated form:

$$\frac{\Delta T}{T_0} = \frac{2\gamma_{ls}}{\Delta H_0}\frac{v_l}{R_p} \tag{2}$$

γ_{ls}, v_l, ΔH_0 and R_p are the liquid–solid interfacial tension, liquid phase molar volume, molar heat of liquid–solid transition and radius of the drop, respectively. The above simple equations are obtained by considering that γ_{ls}, v_l and ΔH_0 are constant in the ΔT interval.

Defay and Prigogine [4] obtained a rigorous relation for the lowering of the triple point temperature. The authors have developed a thermodynamic description of the lowering of the equilibrium temperature between liquid, gas and solid phases in porous media with curved interfaces. They found that the triple point temperature was determined by the curvature of two of the three interfaces. However, in the case of a thermodynamic equilibrium that is only governed by the liquid–solid interface, the treatment of Defay and Prigogine reduces to Kelvin equation.

It is also important to point out that in the theory of Defay and Prigogine, it is assumed that the phase transition energy of a substance held inside a porous material does not change during the transformation and remains equal to the phase transition energy of the undivided liquid.

Later, Brun et al. [6], used the results of Defay and Prigogine to work out a relation between the phase curvature and the shift in triple point temperature by taking into account the variation of the condensate phase transition energy in the porous material. The theoretical treatment allows a quantitative textural characterization of a porous medium through thermal analysis of the liquid–solid transformation occurring inside the medium.

The thermodynamic equilibrium between the phases of a given substance is described by the classical Gibbs–Duhem equation

$$S_i\,\mathrm{d}T - V_i\,\mathrm{d}P_i + n_i\,\mathrm{d}\mu_i = 0 \tag{3}$$

S_i, V_i, n_i and μ_i are entropy, volume, number of moles and chemical potential of phase i; i designates gas (g), liquid (l) or solid (s), respectively.

The interfacial tension, γ_{ij}, between the phases i and j is given by Laplace equation

$$P_j - P_i = \gamma_{ij}\cdot\kappa_{ij} \tag{4}$$

where κ_{ij} refers to the interface curvature between i–j phases. In the case of a planar solid–gas interface, the solid–gas curvature is equal to zero and Eqs. (3) and (4)

applied to solid and liquid phases take the following form:

$$s_l\,dT - v_l\,dP_l + d\mu_l = 0 \quad (5)$$

$$s_s\,dT + d\mu_s = 0 \quad (6)$$

$$P_s - P_l = \gamma_{ls}\cdot\kappa_{ls} \quad (7)$$

where s_i and v_i stand for the molar entropy and molar volume of the substance. At the triple point temperature, the three phases of a pure substance are in equilibrium and thus the three chemical potentials are equal. Combining Eqs. (5)–(7) and taking into account the chemical potentials equality, a relation $T - \kappa_{ls}$ allowing the description of the effect of curvature on the triple point temperature is obtained

$$\Delta H\,dT + v_l T d(\gamma_{ls}\kappa_{ls}) = 0 \quad (8)$$

where, $\Delta H = T(s_s - s_l) = T\Delta s$ is the molar solidification heat of the condensate. Eq. (8) shows that a unique relation exists between temperature and the interface curvature provided that ΔH or Δs is known.

2.1. Relation between pore curvature radius and temperature

Several mechanisms have been proposed to describe the solidification process in a porous body. The most popular ones include

(i) The nucleation by preexisting embryos: in this mechanism, the solidification occurs from critical nuclei that appear spontaneously and grow as the temperature decreases.
(ii) The solidification by progressive penetration of the solid phase: in this case, the solidification proceeds by progressive penetration of the solid phase formed outside the porous body.
(iii) The combination of the above two mechanisms.

Whichever the solidification process retained, the solid–liquid interface is assumed spherical [6] and the interface curvature, κ_{ij}, is given by $(-2/R_n)$, R_n being the radius of the solid phase. The pore radius, R_p, is then obtained by adding to R_n a thickness, d, of the layer of the molecules that are not affected by the solidification (molecules which are in intimate contact with the pore walls). The thickness, d, evaluated by Brun et al. [6] for alumina porous plugs–water systems, was found to be of about 8 Å. Substituting the value of the interface curvature into Eq. (8) and taking T_0 as the normal triple point temperature, we obtain

$$\int_{T_0}^{T}\left(\frac{\Delta s}{2v_l}\right)dT = \frac{\gamma_{ls}}{(R_p - d)} \quad (9)$$

Eq. (9) allows the determination of the radius of pores for each temperature T provided that the variation of Δs, v_l and γ_{ls} with temperature is known. It is worth noting that if Δs and v_l are not depending upon temperature, Eq. (9) is equivalent to Eq. (1). This point will be discussed in more details later.

2.2. Evaluation of the entropy of solidification

The solidification entropy of a solvent held in a porous medium differs from the solidification entropy of the undivided pure solvent. In fact, during solidification, the capillary condensate temperature and the liquid phase pressure differ from those of the bulk condensate and the phase transformation involves rather a liquid–solid interface formation. Moreover, an additional contribution to the solidification entropy is brought by the layer d.

The apparent solidification entropy is then given by [6]

$$\Delta s = (\Delta s)_0 + \int_{T_0}^{T}\frac{C_s - C_l}{T}dT + (P_0 - P_s) \times\left[\left(\frac{\partial v_s}{\partial T}\right)_P - \left(\frac{\partial v_l}{\partial T}\right)_P\right] + \left(\frac{\partial v_l}{\partial T}\right)_P (P_l - P_s) - \frac{2v_l}{R_n}\frac{d\gamma_{ls}}{dT} \quad (10)$$

where, C_s and C_l denote the molar heat capacity at constant pressure of the solid and liquid phases, respectively. P_0 is the normal triple point pressure and P_s the vapor pressure of the undivided solid at temperature T.

Brun et al. [6] have determined the value of γ_{ls} from Eqs. (9) and (10) applied to some porous materials with known pore size distribution. The authors assumed that γ_{ls} is a pore size-independent function that varies linearly with temperature. The following numerical equation was found for water

$$\gamma_{ls}\,(\mathrm{N/m}) = (40.9 + 0.39\Delta T)10^{-3} \quad (11)$$

Finally, inserting Eqs. (10) and (11) into Eq. (9), we obtain the numerical expression of the variation of pore radius with triple point temperature in a porous material saturated with water

$$R_p\,(\mathrm{nm}) = -\frac{64.67}{\Delta T} + 0.57 \quad (12)$$

where $\Delta T = T - T_0$ is the shift in the triple point temperature.

Let us now make some comments on the above derived expressions. Eq. (9) combined with Eq. (10) removes the assumption of the theory of Defay and Prigogine and allows, in principle, the determination of pore size of a porous material by taking into account the variation of enthalpy (or entropy) with temperature and with the curvature of the interface. The variation with temperature is given by the integral and the partial derivative terms in Eq. (10). The last term along with the relation between enthalpy and entropy (see Eq. (8)) reduces in fact to the classical Kelvin equation (Eqs. (1) and (2)). For water liquid–solid transformation, Eqs. (1) and (2) take the following numerical expressions:

$$R_p\,(\mathrm{nm}) = \frac{0.25 + 0.0023\Delta T}{\ln(T_0/T)} \quad (13)$$

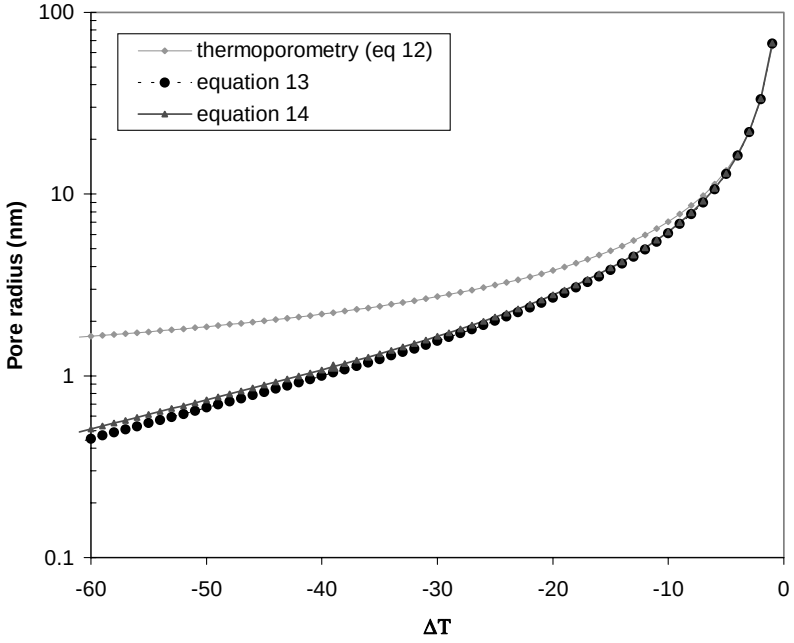

Fig. 1. Comparison of the variation of pore radius with temperature as predicted by Eqs. (12)–(14) in the case of water as a filling solvent.

$$R_p\ (\text{nm}) = -273.15\left(\frac{0.25}{\Delta T} + 0.0023\right) \tag{14}$$

obtained with the following standard values [4,6]: $T_0 = 273.15$ K, $\Delta H_0 = -6012$ J/mol, and $\gamma_{ls}\ (\text{N/m}) = (40.9 + 0.39\Delta T)10^{-3}$.

The predictions of the above Kelvin equations for the variation of pore radius with temperature are compared with those of the general equation (Eq. (12)) in Fig. 1. First note that the pore sizes calculated from Eqs. (13) and (14) are almost identical. In fact, as ΔT is small, $\ln(T/T_0)$ is well approximated by $(\Delta T/T_0)$. The curves are however different from that predicted by Eq. (12). Clearly, the correction introduced by Eq. (12) is only pertinent for $|\Delta T|$ higher than 20°C. Up to $|\Delta T| \approx 20$°C, the predictions of Kelvin equation differ only slightly from the general equation predictions that take into account the variation of entropy with temperature. For high ΔT, Kelvin equation underestimates the pore radius. A 300% divergence could be obtained at $|\Delta T| = 60$°C.

2.3. Equation of the pore radius distribution curve

To determine the pore radius curve distribution, an estimate of the energy of solidification is needed. The theoretical energy of solidification is given by

$$W_{th} = T\Delta s \tag{15}$$

which can be written in the following approximated form for slight variations of Δs with temperature [6]:

$$W_{th} \approx T\Delta s\left[1 - \frac{d\gamma_{ls}}{dT}\frac{\Delta T}{\gamma_{ls}}\right] \tag{16}$$

As mentioned before, a layer of thickness d does not undergo phase transition, so that in a pore with a volume V_{th}, only the volume V_a solidifies and the apparent energy W_a of solidification in the pore is then given by

$$W_a = W_{th}\frac{V_a}{V_{th}} = T\Delta s\left[1 - \frac{d\gamma_{ls}}{dT}\frac{\Delta T}{\gamma_{ls}}\right]\frac{V_a}{V_{th}} \tag{17}$$

Knowing the values of Δs and γ_{ls} (Eqs. (10) and (11)), and applying Eq. (16) to a capillary front of any length gives the following numerical expression for the apparent energy of solidification of water

$$W_a\ (\text{J/g}) = -5.56\times10^{-2}\Delta T^2 - 7.43\Delta T - 332 \tag{18}$$

In practice, the heat (Y) recorded by the calorimeter during the experiment is proportional to the amount of energy involved. Therefore, the volume dV of the pores where the phase transition has occurred is given by

$$dV = k\frac{Y}{W_a}\,d(\Delta T) \tag{19}$$

where k is a factor that depends on the rate of cooling and the weight of the sample. Differentiating Eq. (12) and combining with Eq. (19) gives the distribution curve

$$\frac{\Delta V}{\Delta R_p} = \frac{k}{64.67}\frac{\Delta T^2}{W_a}Y \tag{20}$$

To sum up, Eqs. (12) and (20) allow the calculation of pore size and pore size distribution of a porous material filled with water from the DSC signal corresponding to solidification of water. The use of other solvents is possible but this would require preliminary experiments on materials with known pore size to determine the corresponding γ_{ls}.

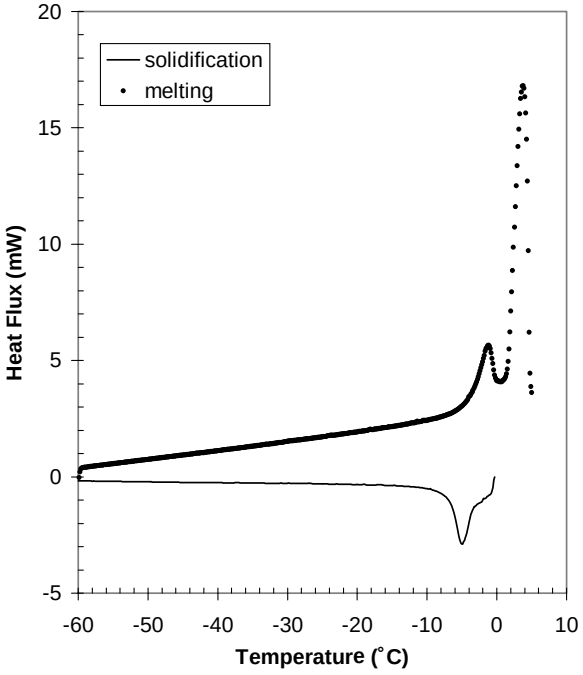

Fig. 2. Melting and solidification thermograms of mesoporous silica (0.5°C/min).

3. Experimental

Hydrogels were prepared from *N*-(2-hydroxypropyl)-methacrylamide (HPMA) by heterophase separation using radical polymerization with a divinyl crosslinking agent. The procedure of synthesis was described elsewhere [14].

The hydrogels used for this study are opaque and the water fraction represents 96% of the swollen weight of the hydrogel [14]. Rheological measurements conducted on a swollen gel exhibited a solid-like behavior characterized by a constant elastic modulus (~200 Pa at 37°C) within the frequency range studied.

DSC measurements: The shift in freezing and melting temperature of water held in mesoporous material was determined by DSC measurements. The DSC apparatus was a Perkin–Elmer DSC7 differential scanning calorimeter equipped with a liquid nitrogen-cooling accessory and calibrated with indium. The sample of about 10–20 mg was put in a sealable aluminum pan and one drop of the solvent was added to maintain the sample in an excess of solvent. Care was taken to avoid the undercooling effect by using the following procedure: the sample was first cooled below the freezing temperature of the pure liquid to −60°C and then heated up and kept isothermally 0.3°C below the normal freezing temperature for 10 min. Thereafter, the pan was cooled down to −60°C at a rate of 0.2°C/min, which is slow enough to maintain the thermodynamic equilibrium. From DSC thermograms and Eqs. (12) and (20), the pore radius distribution curves were obtained.

N_2 physisorption isotherms: Pore radius distribution of the PHPMA hydrogel was calculated from N_2 adsorption/desorption isotherms at 77 K using a Quantachrome Autosorb 1 instrument. The samples were freeze-dried and powdered and then outgassed at 150°C overnight prior to use. The gel at this temperature is thermally stable as was verified by previous thermogravimetric studies. The pore size distribution curve was determined from the desorption isotherm using the model proposed by Barrett, Joyner and Halenda (BJH). Using this technique, mesopore size estimations are obtained from

$$R_p - e\ (\text{Å}) = \frac{-2\gamma V_m}{RT\ \ln(P_0/P)} \tag{21}$$

where γ(is the surface tension of nitrogen at its boiling point, V_m, the molar volume of liquid nitrogen, T, the boiling point of nitrogen and (P/P_0) relative pressure of nitrogen. R_p is the pore radius and e, the thickness of the adsorbed layer remaining on the walls when desorption occurs. The thickness, e, was estimated from a standard curve established by De Boer [15] for silica.

4. Results and discussion

To evaluate the efficiency of the thermoporometry method, experiments were first conducted on a mesoporous silica molecular sieve saturated with water. This material was synthesized in acidic medium using the templating effect of the micellar association with a surfactant, to organize the polymerization of silicate species in acidic conditions (pH 1–1.5) [16,17]. In this particular case a crown ether derived surfactant was used [18]. Fig. 2 shows a typical example of the recorded thermograms. Both melting and solidification thermograms are represented. Due to the procedure described in Section 3, the observed temperature peak was only due to crystallization of water inside the silica mesopores. A temperature peak at −5°C was detected for the kind of water used in this study. On the melting curve, two peaks were detected. A temperature peak corresponding to fusion of "bulk" water at about 4°C and a peak at −1°C for fusion of water inside mesopores. Graham et al. [19] and Kloetstra et al. [20] reported similar phase transition temperatures.

The hysteresis observed between fusion and solidification curves of water inside mesopores was attributed by Brun et al. [6] to the shape of the pores. Indeed, they argued that the solidification and melting thermograms superimpose only in the case where the porous structure is of spherical symmetry. From the difference in melting and freezing temperatures it is then possible to define an empirical shape factor of the pore that characterizes the deviation from sphericity [6].

The average pore radius of the mesoporous silica material obtained from Eqs. (13) and (14) are 12.9 and 14.3 nm, respectively. From Eq. (12), an average pore radius of 13 nm was obtained, value which is in good agreement with the value obtained from Eqs. (13) and (14). The obtained agreement could be explained by the slight

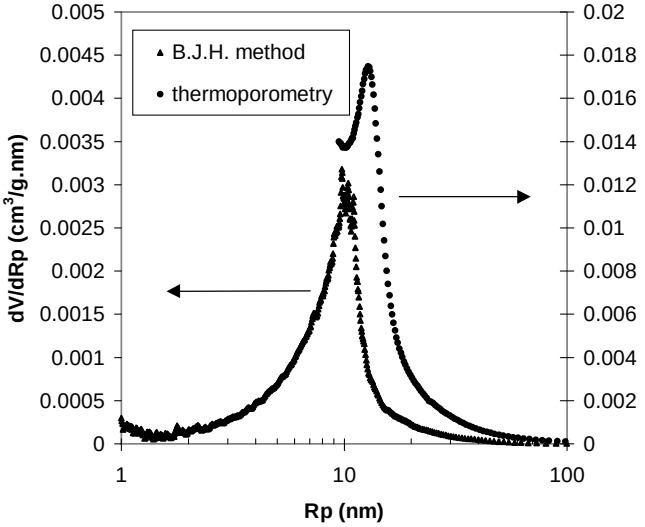

Fig. 3. BJH and thermoporometry distribution curves for mesoporous silica.

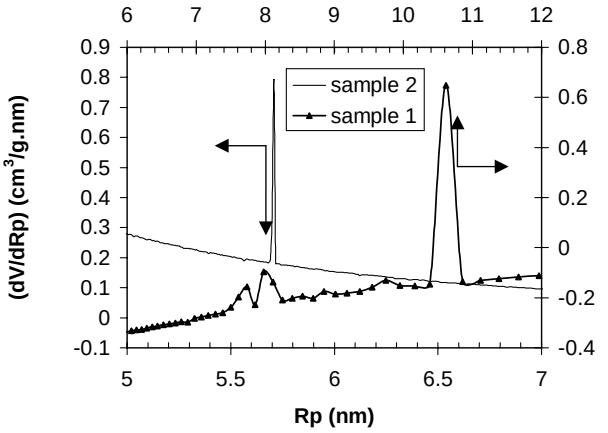

Fig. 5. PHPMA hydrogel pore radius distribution curve (samples 1 and 2).

variation of the solidification energy with temperature and by the pore size range where the three equations yield similar results as shown in Fig. 1. In the case where Δs varies slightly with temperature, Eq. (9) reduces to Eq. (1) (without d) as previously discussed and as shown in Fig. 1. Generally, a porous body with a monodisperse distribution of pore radius and a slight variation with temperature of phase transition energy can be treated by a simple Kelvin equation to estimate the average pore radius.

The comparison between BJH results and thermoporometry is shown in Fig. 3. The two techniques give a maximum pore radius at about 10 and 13 nm, respectively. The slight divergence can be attributed to the different assumptions of the theories used for the two techniques and to the different conditions of analysis. In fact, the silica samples used for both methods are in different states: the adsorption–desorption sample was dried and pretreated at 550°C, whereas the thermoporometry sample was immersed in an excess of water for 1 week. In order to verify if the prolonged contact with water had changed the structure of the mesoporous silica sample, adsorption–desorption measurements were repeated on another sample from the same batch as the one used for thermoporometry and hydrated in excess of water for 1 week. The results did not show any appreciable difference between the two adsorption–desorption distribution curves.

Taking into account the difference in the physical processes involved and the different assumptions in theoretical backgrounds for the two techniques (BJH and thermoporometry) and the fact that BJH method is known to underestimate the pore size [21], the 30% difference in pore radius measured by the two techniques is considered acceptable.

The two techniques were then applied to the PHPMA hydrogel.

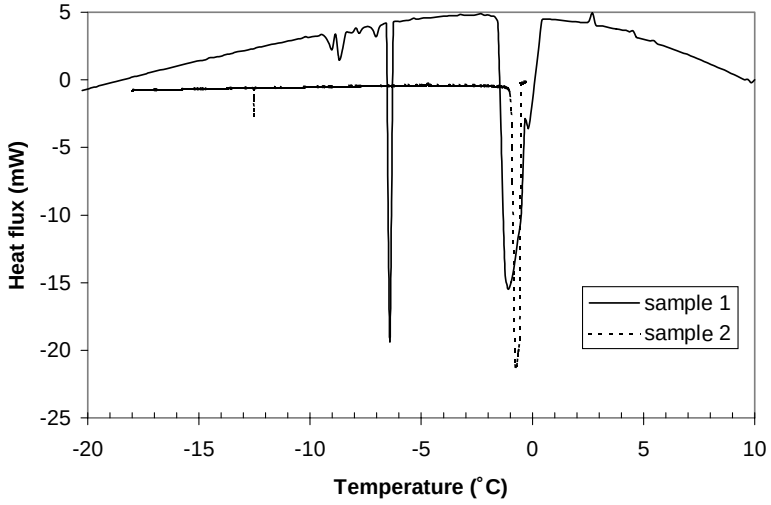

Fig. 4. Solidification thermogram of water contained in PHPMA hydrogel (cooling rate = 0.2°C/min).

Table 1
Pore radius (nm) obtained from thermoporometry and Eqs. (12)–(14) for PHPMA hydrogel

Temperature peak (°C)	R_p (thermoporometry) corresponding to the different peaks of Fig. 5 (Eq. (12))	Eq. (13)	Eq. (14)
−6.4	10.7	9.9	10
−8.7	8.0	7.1	7.2
−9.1	7.7	6.7	6.9
−12.5	5.7	4.7	4.8

4.1. Thermoporometry analysis

The solidification thermograms recorded for PHPMA hydrogel saturated with water are given in Fig. 4. In this figure we have represented two thermograms obtained on two hydrogel samples (sample 1 and 2). The solidification peaks at about 0°C was attributed to the freezing of the excess bulk water. Temperature peaks corresponding to solidification of water inside the mesopores are detected between −15 and −5°C. The mesopore size calculations were made from these latter exothermal peaks.

From the solidification thermogram, pore radius distribution curve was determined. The typical pore radius distribution curve for PHPMA hydrogel saturated by water is illustrated in Fig. 5. Three peaks were obtained from the thermogram of sample 1. The pore size ranges from 7 to 11 nm. Sample 2 gave another pore radius distribution curve. Only one peak was observed and a very narrow distribution was obtained. The average pore radius is of about 5.7 nm, lower than the values found on sample 1. Samples 1 and 2 originate from the same hydrogel (sample 1 from the middle of the hydrogel slice and sample 2 from the edge). The difference between the pore radius values could be attributed to the relative fragility and the structural heterogeneity of this kind of materials. In fact some factors can affect dramatically the network structure and thus can introduce large errors in the experimental results. Some of them are intrinsic to the material and others are experimental:

(i) Heterogeneity of structure: the heterogeneous structure of the hydrogel can lead to different behaviors depending on the place from which the analyzed sample originates.
(ii) The cutting of the sample: to run the thermoporometry experiments a small piece of PHPMA hydrogel was cut and then introduced in the DSC capsule. The procedure of the sample cutting could disorganize the mesoporous structure at least in the zone of cutting. This procedure is done manually and it was not possible to cut the samples in the same way from one experiment to another.
(iii) Compression effect: during sealing of the pan, the cover slightly compresses the sample, and consequently, relatively changes its structure. Previous studies have shown, in fact, that these materials are very sensitive to compression as demonstrated by rheological characterizations performed on these samples with different gaps (different amplitudes of compression) [14].

All these parameters should be responsible of the major sources of variability between the studied samples. Nevertheless, the measured mesopore sizes of the PHPMA hydrogel vary in the interval 5–11 nm. The pore radius was also determined by Kelvin equation (Table 1). As expected, the results are in close agreement to those obtained from Eq. (12).

4.2. Adsorption–desorption pore radius distribution

The BJH pore radius distribution curve of the hydrogel

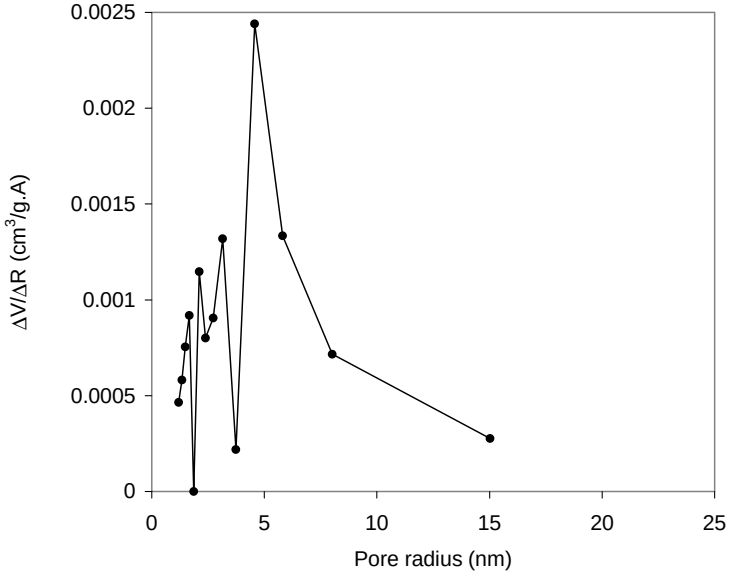

Fig. 6. BJH pore radius distribution curve for PHPMA hydrogels sample 1.

sample 1 is given in Fig. 6. Several peaks are observed. The corresponding average pore radii are between 1.5 and 5 nm. The obtained results are different from those obtained by thermoporometry. BJH experiments gave smaller porous volume and pore radii.

Techniques based on nitrogen physisorption equilibrium require that the sample be thoroughly dried before the experiments. The severity of this pretreatment is likely to be a source of structural damage when the sample is soft and fragile. The freeze-drying process used in this work reduces the specific surface area and may leave traces of adsorbed water so that the surface area values obtained from BET experiments are not representative of the surface in the wet gel. The smaller values of the BJH pore radii suggest that drying also reduces the pore size. It should be stressed that in all samples tested, the values of pore radius obtained by the BJH method are always smaller than those measured by thermoporometry. This is in particular true for the mesoporous silica sample (Fig. 3). Such a result is in line with the conclusions of Ravikovitch et al. [21] who found that the BJH model underestimates the average pore size in MCM-41 mesoporous materials. In addition, the nitrogen physisorption isotherms techniques are limited in the range of pore size which can be measured and do not yield precise estimates of pore radii higher than some tens of nanometers. It is also significant that with the two types of methods used in this work, the pore volume estimates were very different. The significantly lower values obtained with N_2 physisorption suggest that the drying pretreatment induces a collapse of the pore structure, whereas in thermoporometry the sample is swollen by the solvent during measurement and all pores remain open.

Although the thermoporometry technique for hydrogels presents some advantage in comparison to other methods, some factors can affect its reliability. The mains ones are summarized below.

The equation governing the thermoporometry was obtained by using some approximations, which are only valid for small enough ΔT. Moreover, thermoporometry concept does not take into account the effect of stresses exerted on the pore wall by ice when it penetrates into the network. These stresses may introduce a supplementary pressure that can modify the thermodynamic equilibrium and may also cause sample damage [13]. Indeed, the crystal inside the mesopore can grow by pushing the neighboring pores inducing thus a disorganization of porous structure.

The solidification process retained in thermoporometry is either the progressive penetration of front crystal or the heterogeneous nucleation. If the first mentioned process is predominant, thermoporometry provides a measure of the pore-neck size rather than pore radius, so that the pore size is falsely interpreted. Moreover, the front is supposed to be spherical, which is a rough approximation especially for small pores. For these reasons, some precautions should be taken in the interpretation of the results obtained from this technique. Nevertheless and even if the results have to be considered carefully, thermoporometry remains the most reliable method for studying the mesoporous fragile structures, in their working conditions.

5. Concluding remarks

This study has revealed the big difficulty in analyzing the structure of soft and fragile materials like hydrogels. The original structure of this kind of materials may undergo a structural modification if particular precautions are not taken. Our studies have demonstrated the usefulness of thermoporometry in probing the structure of soft gels in aqueous solvent. In contrast to the classical techniques (like BJH that underestimates the pore size), thermoporometry allows the determination of the porous dimensions in the presence of a solvent that swells the material. As the mesoporous structure of these materials changes with the swelling, thermoporometry provides a unique method for the porous characterization of the hydrogels.

It was also demonstrated that for small variations of temperature (small shift in freezing point with curvature), Kelvin equation for capillary condensation could be extended to solid–liquid transformation to provide an acceptable estimation for the pore radius of porous materials. For large variations in temperature, correction terms that take into account the variation of entropy and interfacial tension with temperature should be considered.

Acknowledgements

This work was supported by Organogel Canada Ltée.

References

[1] Korsmeyer RW. In: Tarcha PJ, editor. Polymers for controlled drug delivery, Boca Raton, FL: CRC Press, 1990. p. 15.
[2] Woerly S. Mat Sci For 1997;250:53–68.
[3] Kuhn W, Peterli E, Majer H. J Pol Sci 1955;16:539–48.
[4] Defay R, Prigogine I, Bellemans A. Surface tension and adsorption, New York: Wiley, 1966.
[5] Quinson JF, Brun M. In: Unger KK, editor. Characterization of porous solids, Amsterdam: Elsevier, 1988. p. 307.
[6] Brun M, Lallemand A, Quinson JF, Eyraud C. Thermo Acta 1977;21:59–88.
[7] Quinson JF, Dumas J, Serughetti J. J Non-Cryst Sol 1986;79:397–404.
[8] Brun M, Quinson JF, Benoist L. Thermo Acta 1981;49:49–52.
[9] Brun M, Quinson JF, Spiz R, Bartholin M. Makro Chem 1982;183:1523–31.
[10] Neffati R, Apekis L, Rault J. J Ther Anal 1998;54:741–52.
[11] Quinson JF, Tchipkam N, Dumas J, Bovier C, Serughetti J, Guizard C, Larbot A, Cot L. J Non-Cryst Sol 1988;99:151–9.
[12] Ehrburger-Dolle F, Misono S. Carbon 1992;30:31–40.
[13] Scherer GW. J Non-Cryst Sol 1993;155:1–25.
[14] Woerly S, Pinet E, de Robertis L, Bousmina M, Laroche G, Roitbak T, Vargova L, Sykovà E. J Biomat Sci Poly Ed 1998;9:681–712.
[15] Gregg SJ, Sing KSW. Adsorp, surface area and porosity, 2nd ed. London: Academic Press, 1982.

[16] Kresge CT, Leonowicz ME, Roth WJ, Vartuli JC, Beck JS. Nature 1992;359:710.
[17] Firouzi A, Kumar D, Bull LM, Besier T, Sieger P, Huo Q, Walker SA, Zasadzinski JA, Glinka C, Nicol J, Margolese D, Stucky GD, Chmelka BF. Science 1995;267:1138.
[18] Danumah C, Zaidi SMJ, Voyer N, Giasson S, Kaliaguine S. Studies in Surface Science and Catalysis 1998;117:281.
[19] Graham NB, Zulfiqar M, Nwachuku NE, Rashid A. Polym 1990;31:909–16.
[20] Kloetstra KR, Zandbergen HW, Van Koten MA, Van Bekkum H. Catalysis Letters 1995;33:145–56.
[21] Ravikovitch PI, Wei D, Chueh WT, Haller GL, Neimark AV. J Phys Chem B 1997;101:3671–9.